Thermal and electrical transport in the spin density wave antiferromagnet $CaFe_4As_3$

M. S. Kim,[1,2] Z. P. Yin,[2,3] L. L. Zhao,[4] E. Morosan,[4] G. Kotliar,[3] and M. C. Aronson[1,2]

[1]*Condensed Matter Physics and Materials Science Department, Brookhaven National Laboratory, Upton, New York 11973-5000, USA*

[2]*Department of Physics and Astronomy, Stony Brook University, Stony Brook, New York 11794-3800, USA*

[3]*Department of Physics and Astronomy, Rutgers University, Piscataway, New Jersey 08854, USA*

[4]*Department of Physics and Astronomy, Rice University, Houston, Texas 77005, USA*

(Received 17 January 2011; revised manuscript received 2 June 2011; published 5 August 2011)

We present here measurements of the thermopower, thermal conductivity, and electrical resistivity of the newly reported compound $CaFe_4As_3$. Evidence is presented from specific heat and electrical resistivity measurements that a substantial fraction of the Fermi surface survives the onset of spin density wave (SDW) order at the Néel temperature $T_N = 88$ K and its subsequent commensurate lock-in transition at $T_2 = 26.4$ K. The specific heat below T_2 consists of a normal metallic component from the ungapped parts of the Fermi surface and a Bardeen-Cooper-Schrieffer (BCS) component that represents the SDW gapping of the Fermi surface. A large Kadowaki-Woods ratio is found at low temperatures, showing that the ground state of $CaFe_4As_3$ is a strongly interacting Fermi liquid. The thermal conductivity κ of $CaFe_4As_3$ is an order of magnitude smaller than those of conventional metals at all temperatures, due to a strong phonon scattering. The thermoelectric power S displays a sign change from positive to negative indicating that a partial gap forms at the Fermi level with the onset of commensurate spin density wave order at $T_2 = 26.4$ K. The small value of the thermopower S and the enhancements of the resistivity due to gap formation and strong quasiparticle interactions offset the low value of the thermal conductivity κ, yielding only a modest value for the thermoelectric figure of merit $\mathcal{Z} \leqslant 5 \times 10^{-6}$ K^{-1} in $CaFe_4As_3$. The results of *ab initio* electronic structure calculations are reported, confirming that the sign change in the thermopower at T_2 is reflected by a sign change in the slope of the density of states at the Fermi level. Values for the quasiparticle renormalization Z are derived from measurements of the specific heat and thermopower, indicating that as $T \to 0$, $CaFe_4As_3$ is among the most strongly correlated of the known Fe-based pnictide and chalcogenide systems.

DOI: 10.1103/PhysRevB.84.075112 PACS number(s): 72.15.Jf, 72.15.Eb, 75.30.Fv

I. INTRODUCTION

Although thermoelectric materials have received enduring attention over the past half century for their ability to convert thermal energy to electrical energy and vice versa, the growing need to develop new materials with enhanced properties for applications has led to a renewed interest in recent years.[1] The potential performance of a given thermoelectric material is expressed in terms of the thermoelectric figure of merit $\mathcal{Z} = S^2/\rho\kappa$, where S is the thermoelectric power, ρ is the electrical resistivity, and κ is the thermal conductivity. High thermoelectric power must be combined with low thermal conductivity and low electrical resistivity to optimize the figure of merit. Large values of $\mathcal{Z}$ have been observed in the filled skutterudites AT_4Sb_{12} (A = rare earths or alkaline earth metals, T = transition metals), which combine large values of the thermopower S, which can be as large as 10–100 μV/K, with low thermal conductivity κ, as small as a few W/K-m.[2,3] The low κ of these systems reflects an unusually small phonon contribution, originating with enhanced scattering of heat-carrying phonons from the low-energy rattling and tunneling modes of filler "A" atoms in the T_4Sb_{12} cagelike structures characteristic for these compounds.[4,5] Consequently, it is potentially of great interest to identify and explore other classes of correlated materials that similarly form in open and cagelike structures.

Recently, a new Fe-As system, $CaFe_4As_3$, has been reported,[6,7] which crystallizes in orthorhombic structure (space group $Pnma$). In this structure, the Ca atoms are confined inside nearly rectangular tunnels, oriented along the b axis, whose walls are constructed from a network of Fe-As tetrahedra which are similar to the FeAs planes in the layered iron-pnictide superconductors. The combination of confined Ca atoms and the open structure of the FeAs framework in $CaFe_4As_3$ is reminiscent of the cages in the filled skutterudites RFe_4As_{12} (R = Ce and Pr),[8,9] and it is possible that here too a low thermal conductivity might be realized. We note as well that large thermopowers are generally found in metals where strong correlations lead to enhanced densities of states near the Fermi level. $CaFe_4As_3$ undergoes an antiferromagnetic transition at $T_N = 88$ K, which has been classified as an incommensurate spin density wave (SDW).[10,11] The SDW becomes commensurate with the underlying lattice below a second transition that occurs at $T_2 = 26.4$ K. However, the SDW does not appear to gap the entire Fermi surface, since metallic Fermi liquid behavior is found at the lowest temperatures, where the electrical resistivity $\rho(T) = \rho_0 + AT^2$ and the electronic specific heat $C_{el} = \gamma T$. Intriguingly, the Kadowaki-Woods ratio A/γ^2 is very large, approaching a value of 55×10^{-5} $\mu\Omega$ cm mol^2 K^2 mJ^{-2}.[7] This suggests that the quasiparticles of the Fermi liquid have substantial interactions, at a level that is comparable to those realized in the heavy-fermion compounds. The possibility of a small thermal conductivity, derived from the confinement of the Ca atoms, and the possibility of strong enhancement of the density of states at low temperatures, suggested by the large Kadowaki-Woods ratio, make $CaFe_4As_3$ a promising candidate for a large thermoelectric figure of merit. Accordingly, we present here measurements of the thermal and electrical transport properties of single crystals of $CaFe_4As_3$, which together with *ab initio*

calculations of the electronic structure probe not only the character of the quasiparticles forming the ground state but also the impact of the SDW transitions on the electronic structure.

II. EXPERIMENTAL DETAILS

Single crystals of $CaFe_4As_3$ were grown from a Sn flux, forming in a rodlike morphology with the crystallographic b axis along the rod axis. Details of the sample preparation are described in Ref. 7. Using the thermal transport option (TTO) of a Quantum Design physical property measurement system (PPMS) over the range of temperatures with $2\,K < T < 300\,K$, the thermal conductivity $\kappa(T)$, thermoelectric power $S(T)$, and resistivity $\rho(T)$ were simultaneously measured on a $0.5 \times 0.5 \times 3\ mm^3$ sample using a two-probe method, where the temperature gradient across the sample was always less than 3% of the background temperature during the measurement and an AC current of 1 mA with frequency of 17 Hz was applied for the resistivity measurement. Specific-heat measurements were also carried out using the thermal relaxation technique implemented on the PPMS for $5\,K < T < 150\,K$.

III. EXPERIMENTAL RESULTS AND DISCUSSION

The filled circles in Fig. 1(a) show the temperature dependence of the thermal conductivity κ, measured with the heat flow along the b axis of a single crystal of $CaFe_4As_3$. The temperature dependence of the electrical resistivity $\rho(T)$

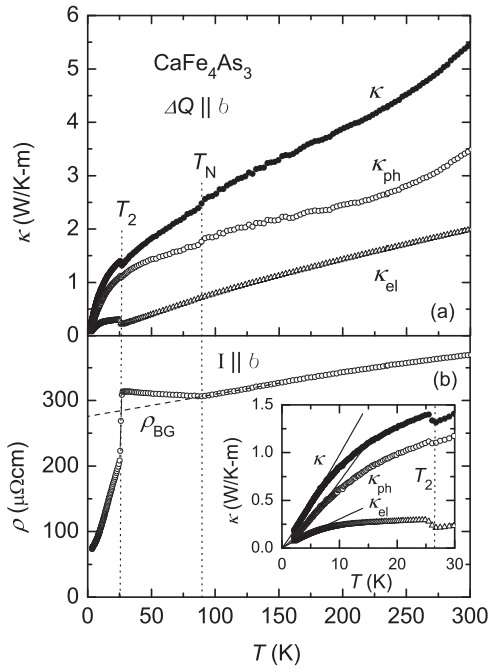

FIG. 1. (a) Temperature dependencies of the measured thermal conductivity κ along the b axis, the electron contribution of the thermal conductivity κ_{el} estimated from the Wiedemann-Franz law, and the phonon contribution of the thermal conductivity $\kappa_{ph}(=\kappa - \kappa_{el})$; see text. (b) Temperature dependence of the resistivity ρ along the b axis (open circles). The dashed line indicates ρ_{BG} which is determined from a linear extrapolation of the data above T_N. The inset shows κ, κ_{el}, and κ_{ph} below 30 K.

is presented in Fig. 1(b), showing an overall metallic character, with a sharp drop at T_2 and a slope discontinuity at T_N. The electronic contribution to the thermal conductivity κ_{el} was determined using the Wiedemann-Franz law $\kappa_{el} = L_0 T/\rho$, where L_0 is the Sommerfeld value 2.45×10^{-8} WΩ/K^2 for the Lorenz ratio $L = \rho\kappa/T$. The phonon contribution κ_{ph} was subsequently determined as the difference between κ and κ_{el}. κ, κ_{el}, and κ_{ph} are compared in Fig. 1(a). We note that values for κ above ~200 K are likely to be ~10%–30% higher than the actual values, due to systematic discrepancies in the PPMS/TTO radiation corrections.[12,13]

The overall thermal conductivity κ of $CaFe_4As_3$ is an order of magnitude smaller at all temperatures than the values found in conventional metals, which are typically ≈10–30 W/K-m. However κ is comparable to the values measured in the filled skutterudites AT_4X_{12}.[3,8,9,14] For example, κ of RFe_4As_{12} (R = Ce and Pr) is no more than 3 ~ 4 W/K-m at all temperatures,[8,9] comparable to the values found in $CaFe_4As_3$ above T_N [Fig. 1(a)], and as much as a full order of magnitude larger than at the lowest temperatures. By analogy to the filled skutterudites, the characteristically small value of κ in $CaFe_4As_3$ can be attributed to its cagelike structure, described above.[6,7] The equivalent isotropic atomic displacement parameter (ADP) of the Ca atoms is more than 40% larger than the averaged equivalent isotropic ADP of the Fe and As atoms in $CaFe_4As_3$,[6] and is comparable to the amplitudes of motion realized in the skutterudites, where the ADPs of the filler atoms are ≈30% larger than those of the other atoms.[15] If the low thermal conductivity observed in $CaFe_4As_3$ arises from the rattling of Ca atoms in the open tunnel-like structure, then the phonon mean-free path should be comparable to either the 6 Å cage dimension or to the 3.7 Å nearest Ca-Ca separation distance. We have estimated the phonon mean-free path d using the expression $\kappa_{ph} = \frac{1}{3} C_v v_s d$, where C_v at 300 K is 189 J/mol K, a Debye temperature θ_D is taken from the ADP of $CaFe_4As_3$ as 328 K, and the averaged sound velocity v_s is estimated from the Debye model to be 2784 m/s.[16] The total mean-free path $d \sim 12$ Å, which is substantially larger than either the dimension of the tunnel-like structure in $CaFe_4As_3$ or the spacing of the Ca ions contained in the cage. We conclude that the small thermal conductivity likely does not originate with a rattling mode, but instead with strong phonon scattering due to the complicated crystal structure and 32-atom unit cell, with multiple Fe and As site symmetries.

Further evidence for the strong phonon scattering comes from the temperature dependence of κ, which displays a broad shoulder centered around 30 K in $CaFe_4As_3$. Ordinarily, a broad maximum in κ_{ph} is expected at $T \approx \theta_D/10$, resulting from the crossover between phonon-boundary and/or phonon–point defect scattering at low temperatures ($T \ll \theta_D/10$) and phonon-phonon Umklapp scattering at high temperatures ($T \gg \theta_D/10$). In principle, the absence of a maximum in $\kappa(T)$ in $CaFe_4As_3$ might be ascribed to particularly strong phonon scattering from pointlike defects. However, the broad maximum is found even in polycrystalline filled skutterudites, where defects are expected to be plentiful.[3] A shoulder in $\kappa(T)$ is found only in skutterudites with small filler atoms,[3,17] whose large amplitude rattling leads to particularly strong phonon scattering. The shoulder observed in $\kappa(T)$ in $CaFe_4As_3$

implies that the phonon scattering is very strong here as well.

The temperature dependencies of the thermal conductivities κ and the electrical resistivity ρ reveal the presence of a SDW transition into an antiferromagnetically ordered state below the Néel temperature $T_N = 88$ K. Recent neutron diffraction measurements confirm that the 88 K transition in $CaFe_4As_3$ is indeed to an incommensurate SDW state.[10,11] Figure 1(a) shows that κ_{el} decreases approximately linearly as the temperature is reduced, and like $\rho(T)$ displays a weak anomaly at T_N. Measurements carried out on charge density wave (CDW) systems $K_{0.3}MoO_3$ and $(TaSe_4)_2I$ (Ref. 18) find only a small cusp in κ_{ph} but not in κ_{el} with the onset of the lattice distortion associated with the CDW, just as we observe at the SDW transition in $CaFe_4As_3$. The softening of the phonons that drive CDWs, and to a lesser extent SDWs, is thought to be responsible for the reduced values of κ_{ph} found in the ordered state $T \leqslant T_N$ [Fig. 1(a)].[19] Given the complexity of the Fermi surface of $CaFe_4As_3$,[11] we can expect that SDW formation will lead only to a partial gapping of the Fermi surface, resulting in a decreased density of states and a higher electrical resistivity in the ordered phase. This explains the initial increase in $\rho(T)$ below T_N in $CaFe_4As_3$, which is much as is found in Cr near its 311 K transition to an incommensurate SDW state.[20] However, the remaining states at the Fermi surface ultimately lead to the resumption of a metallic temperature dependence of the resistivity below T_2 [Fig. 1(b)], previously reported by Zhao *et al.*[7] A second resistivity anomaly is found at $T_2 = 26.4$ K, where the SDW becomes commensurate.[10,11] κ_{el} increases sharply at T_2 [inset of Fig. 1(b)], but a monotonic decrease in κ, κ_{el}, and κ_{ph} is found at the lowest temperatures. In combination with the decidedly metallic electrical resistivity [Fig. 1(b)], we conclude that the SDW gapping of the Fermi surface is only partial, and that the residual density of states at the Fermi level leads to normal metallic behavior as $T \to 0$.

The temperature dependence of the thermoelectric power $S(T)$ depicted in Fig. 2 also confirms the strong phonon scattering in $CaFe_4As_3$. In general, the thermoelectric power S is the sum of the phonon drag and diffusion terms, S_g and S_d, respectively. Phonon drag in metals leads to a prominent peak in S_g at $\sim \theta_D/5$, which is caused by a crossover between different phonon scattering mechanisms at higher and lower temperatures.[21] The small arrow in Fig. 2 shows at most a vanishingly small peak in $S(T)$ near 70 K $\simeq \theta_D/5$, indicating that the phonon-drag peak and indeed $S_g(T)$ itself are suppressed in $CaFe_4As_3$, presumably by the strong phonon scattering. Consequently, we take $S_g \ll S_d$, so that $S = S_g + S_d \sim S_d$ for $CaFe_4As_3$.

The thermopower S is surprisingly small in $CaFe_4As_3$, considering the rather large magnitude of the electrical resistivity ρ. Nonetheless, the magnitudes of S and ρ are comparable to those found in $CaFe_2As_2$, where $\rho \simeq 0.4$ mΩ cm and $S \simeq 1$–2 μV/K above the structure/magnetic transition temperature at 170 K.[22] This correspondence suggests that the small magnitude of S in both compounds results from a near balance of the electron and hole concentrations, and this result is confirmed for $CaFe_2As_2$ in first-principles electronic structure calculations.[23] We will show below that our own electronic structure calculations, carried out using DFT, support a similar conclusion in $CaFe_4As_3$, and that this particle-hole symmetry is expected in compounds with SDW transitions.

Above T_2, S is positive with a broad maximum, reaching a value of 3.3 μV/K at $\approx$170 K. Only a vanishingly weak anomaly is found at T_N, while a sharp drop is found at T_2 where S changes sign from positive to negative with decreasing temperature. S is proportional to the energy derivative of the density of states (DOS). The sign change of S at T_2 indicates that a drastic change of the DOS accompanies the commensurate SDW transition at T_2, and we will show below that this too is consistent with the electronic structure calculations.

Figure 3 shows the temperature dependence of the specific heat C_p/T measured for $CaFe_4As_3$ for $5 < T < 150$ K. C_p/T is not linear in T^2 for $T \leqslant 35$ K, suggesting that there may be an electronic and magnetic component of the specific heat for $T \leqslant T_2$, in addition to the phonon contribution. To investigate this possibility, we have modeled C_p as the sum of a Sommerfeld term $\gamma_g T$, a phonon contribution $C_{ph} = \beta T^3$, and a Bardeen-Cooper-Schrieffer (BCS) term $C_{BCS} = A_g \exp(-\Delta/T)$ that reflects the temperature depen-

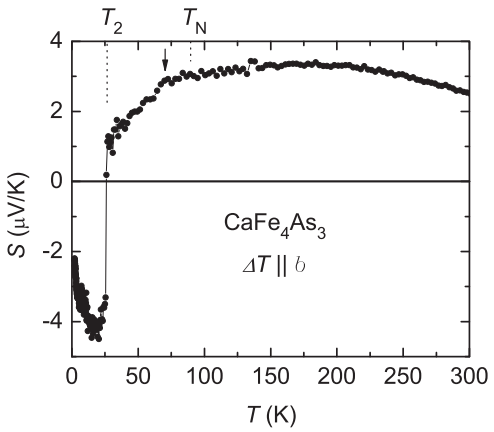

FIG. 2. Temperature dependence of the thermoelectric power S with the heat flow along the b axis.

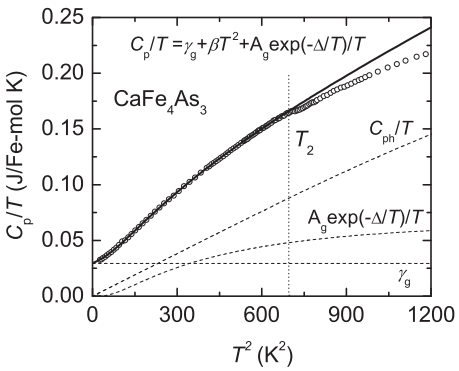

FIG. 3. The plot of C_p/T vs T^2 below 35 K. The solid line indicates the fit of the expression described in the figure, below T_2. Dashed lines indicate the phonon specific heat divided by T, C_{ph}/T, which is estimated using Debye model with Debye temperature ($\theta_D =$ 312 K) calculated from obtained β, the Sommerfeld specific heat γ_g, and BCS component divided by T, $A_g \exp(-\Delta/T)/T$.

dence in the specific heat resulting from the formation of the SDW gap:

$$C_p/T = C_{el}/T + C_{ph}/T + C_{BCS}/T$$
$$= \gamma_g + \beta T^2 + A_g \exp(-\Delta/T)/T.$$

The best fit to the data for $T \leqslant T_2$ is shown in Fig. 3, where the three different components of the fit are compared. The parameters of this fit are $\gamma_g = 0.03$ J/Fe-mol K^2, $\beta = 1.27 \times 10^{-4}$ J/Fe-mol K^3, $A_g = 9.37$ J/Fe-mol K, and $\Delta = 52.80$ K. The ratio $\Delta/k_B T_2 = 2.0$ is very similar to the value of 2.3 found for the incommensurate SDW in Cr,[20] and is also close to the minimum value of 1.764 found in the two-band model of itinerant antiferromagnetism.[24] We note that the Debye expression using the same value of $\theta_D = 312$ K determined from this fit also describes the specific heat above T_N well [Fig. 4(a)], where the electronic and magnetic contributions are expected to be very small. This value of $\theta_D = 312$ K is also in good agreement with the value of 328 K that was determined from the ADP. The internal consistency of these different estimates of θ_D gives added weight to our conclusion that a broad peak at ~40 K in $C_p - C_{ph}$ is electronic and magnetic in origin, and does not reflect anomalous features in the phonon density of states that are not described by the Debye model. The electronic and magnetic part of the specific heat $C_p - C_{ph}$ displays a sharp peak at T_N [Fig. 4(a)], although only a weak peak marks the onset of commensurate SDW order at T_2 (Fig. 3). Both SDW ordering anomalies are superposed on the broad peak that is centered near ~40 K. Although we do not show the data here, this broad peak is unchanged when magnetic fields as large as 9 T are applied, indicating that it is not likely to be a Schottky anomaly. Its insensitivity to fields suggests instead an intrinsic electronic excitation of the incommensurate SDW with an energy scale $\Delta \approx 0.45\, k_B T_N$.

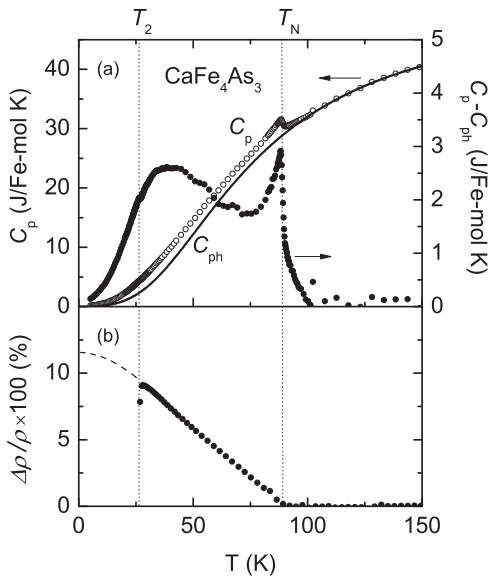

FIG. 4. (a) Temperature dependencies of the specific heat C_p (open circles), the phonon contribution C_{ph} estimated from the Debye model (solid line), and their difference, the electronic specific heat $C_p - C_{ph}$ (filled circles). (b) Temperature dependence of the ratio $\Delta\rho/\rho \times 100$, extrapolated below T_2 (dashed line).

Electrical resistivity measurements can be used to estimate how much of the Fermi surface in $CaFe_4As_3$ is gapped by the incommensurate and commensurate SDW transitions. Analyses carried out in other SDW systems have used high magnetic fields to collapse the SDW gap, revealing the underlying background resistivity ρ_{BG} of the gapless state.[25,26] This approach is not possible in $CaFe_4As_3$, where the small measured magnetoresistance[7] implies that very large fields would be required to close the SDW gap. Instead, we determine ρ_{BG} in $CaFe_4As_3$ by a linear extrapolation of the measured resistivity for $T \geqslant T_N$, as shown in Fig. 1(b). We subtracted this estimate of ρ_{BG} from ρ, and normalized by ρ to obtain $(\rho - \rho_{BG})/\rho = \Delta\rho/\rho$, which represents the percentage change in the resistivity that can be associated with SDW formation. This is in turn proportional to the ratio of the Fermi surface volumes in the gapped and ungapped states.[25] The temperature dependence of $\Delta\rho/\rho$ is plotted in Fig. 4(b). $\Delta\rho/\rho$ increases in an order-parameter-like fashion below T_N, extrapolating to a value of ≈10% as $T \to 0$ in the absence of the commensurate transition at T_2. This result implies that the incommensurate SDW in $CaFe_4As_3$ gaps about 10% of the Fermi surface.

Our analysis of the specific heat is also consistent with a Fermi surface in $CaFe_4As_3$ that is only partially gapped by SDW formation. We note that γ_g is slightly enhanced, indicating that the quasiparticles that survive the Fermi surface gapping at both T_N and T_2 have substantial interactions that increase their effective masses and lead to the heavy-fermion behavior already noted for $CaFe_4As_3$.[7] We point out that the $T = 0$ value of the quasiparticle gap associated with SDW formation, Δ, is very similar to the 40 K electronic energy scale deduced from the broad peak in the specific heat $C_p - C_{ph}$ above T_2, suggesting a common origin.

Our measurements confirm the general scenario of Fermi surface gapping that is accomplished by incommensurate SDW formation at T_N, followed by a second transition at T_2, where the SDW becomes commensurate with respect to the underlying lattice. The temperature dependence of the specific heat below T_2 is well described within the BCS theory, and we present evidence for a possible collective mode of the SDW gapped state, having a characteristic energy of ≈0.25Δ.The overall success of this analysis, which assumes an itinerant nature for the magnetism in $CaFe_4As_3$, is somewhat surprising, considering that the neutron scattering measurements found a rather large Fe moment in the paramagnetic state. Inelastic scattering experiments are needed to assess the possibility that Δ instead represents an anisotropy gap in the transverse spin excitations, suggestive of a more localized picture of the magnetism.

We will combine these experimental results with electronic structure calculations to elucidate the strength of the correlations in $CaFe_4As_3$, and to provide a phenomenological understanding of the thermal and electrical properties described above. The electronic structure of $CaFe_4As_3$ was first considered in its paramagnetic state.[6] It was subsequently shown[11] that the large unit cell leads to a much larger Fermi surface with a different topology than those found in the 1111 and 122 families of iron pnictides. Our analysis shows that the strength of the correlations in $CaFe_4As_3$, at least in the SDW phase, is substantially higher than in other iron pnictides

such as the 1111 and the 122 families, while being comparable to the 111 and 2322 families, as well as to the 11 family of iron chalcogenides.[27,28] Our calculations correctly reproduce the sign change in the density of states at the Fermi level, predicted by the temperature dependence of the thermopower. Finally, we ascribe the observed low thermoelectric coefficient to a substantial particle-hole symmetry present near the Fermi level, and suggest compositional modifications that may improve the thermoelectric performance of $CaFe_4As_3$.

An alternative interpretation of the thermoelectric power data can be provided within a picture where all the electrons are itinerant. In this view, all five Fe d bands are important in the electronic structure of $CaFe_4As_3$, and we assume that the correlation strength is intermediate. By this we mean that the correlations are not large enough to make the material insulating, but also not so small that the wave function renormalization Z is less than 0.5. These initial assumptions are consistent with previous calculations on $LaO_{1-x}F_xFeAs$,[29] which found a mass renormalization between 3 and 5 ($Z \sim 0.2$–0.3), in good agreement with subsequent optical experiments.[30] Rather than calculating Z from first principles for $CaFe_4As_3$, we extract it from an analysis that combines the results of the thermopower and specific-heat measurements described above with *ab initio* electronic structure calculations carried out in both the paramagnetic and ordered states. The unit cell needed to describe the incommensurate order for $T_2 \leqslant T \leqslant T_N$ is prohibitively large, so we will restrict our calculations to the paramagnetic state with $T \geqslant T_N$ and the commensurate SDW state with $T \leqslant T_2$.

We performed density functional theory (DFT) calculations in both the low-temperature SDW and the high-temperature paramagnetic phases of $CaFe_4As_3$. The calculation is done using the projector augmented wave (PAW) method[31,32] as implemented in VASP[33] and the PBE exchange correlation functional.[34] The lattice constants $a = 11.852$ Å, $b = 3.7352$ Å, and $c = 11.5490$ Å as well as the atomic coordinates are taken from the 15 K SDW state.[6] For the paramagnetic state, we use a $8 \times 24 \times 8$ dense mesh and an energy cutoff of 300 eV. To simulate the low-temperature SDW state with a $Q = (0, 3/8\,\pi/b, 0)$ wave vector,[10] we use a $1 \times 8 \times 1$ supercell of the PM unit cell and perform a non-collinear magnetic calculation using a $6 \times 2 \times 6$ mesh and an energy cutoff of 250 eV. The magnitude and arrangement of the magnetic moments in our calculations agree well with those deduced from experimental measurements.[10]

The density of states that results from these calculations in both the high-temperature paramagnetic state and the low-temperature SDW state is presented in Fig. 5. We note with interest that the energy derivative of the density of states $N'(\varepsilon)$ changes sign from negative in the paramagnetic phase to positive in the SDW phase. The density of states at the Fermi level is approximately twice as large in ungapped and paramagnetic $CaFe_4As_3$ as it is in SDW $CaFe_4As_3$, indicating that the SDW gap has removed a large fraction of the high-temperature Fermi surface.

It is our intention to combine experimental measurements of the thermopower $S(T)$ with these DFT calculations of $N(\varepsilon)$ and its energy derivative $N'(\varepsilon)$ to estimate the quasiparticle renormalization factor Z_S. An independent determination of $Z = Z_\gamma$ can be extracted from the Sommerfeld coefficient γ_g,

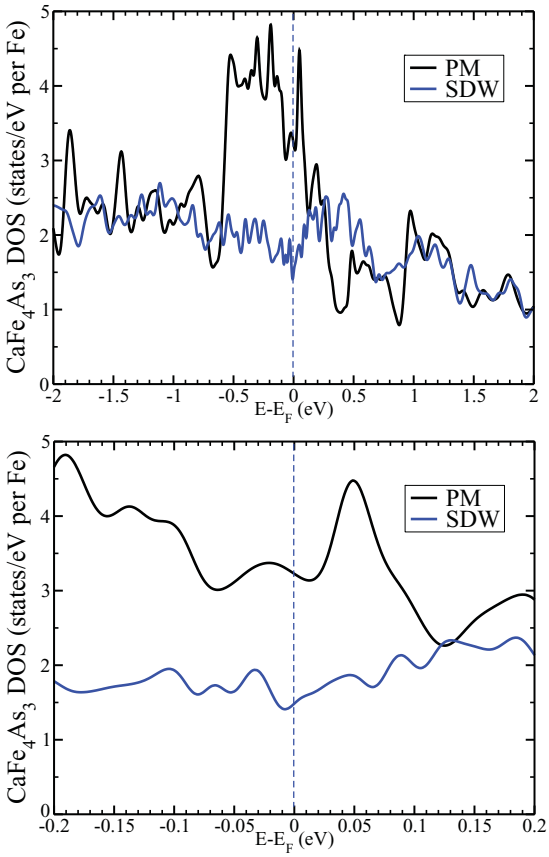

FIG. 5. (Color online) Upper panel: The density of states (DOS) for both the high-temperature paramagnetic (PM) phase and low-temperature SDW phase of $CaFe_4As_3$. An expanded view near the Fermi level is presented in the lower panel.

although this is only possible in the SDW phase since the large phonon contribution to the specific heat C_p prohibited an accurate determination of γ_g in the paramagnetic state. We obtain expressions for the thermopower S and Sommerfeld coefficient γ_g with the aid of the corresponding local Fermi equations,[35] ignoring the asymmetry in the self-energy,[36] and estimating the slope of the value of a transport function Φ_{ε_F} from the derivative of the density of states calculated using DFT. Z is understood to be an average quasiparticle renormalization weight.

$$S = -\frac{k_B}{|e|}\frac{k_B T}{Z_S}\frac{\Phi'(\varepsilon_F)}{\Phi(\varepsilon_F)}\frac{E_2^1}{E_0^1}, \tag{1}$$

$$\gamma_g = \frac{\pi^2}{3}\frac{k_B^2}{Z_\gamma}N(\varepsilon_F), \tag{2}$$

where $k_B/|e| = 8.6 \times 10^{-5}$ V/K, $N(\varepsilon_F)$ is the density of states at the Fermi energy ε_F, and $E_2^1 = 1.75$ and $E_0^1 = 0.82$.[35] The experimental input is listed in Table I, and consists of the experimental value of the SDW value of $\gamma_g(T \to 0)$ as well as two values for the temperature derivative of S, one for the paramagnetic state, which we approximate as $S(T_N)$, and one which represents the gapped SDW state, which we set equal to $S(T_2)$. Both are subsequently extrapolated to $T = 0$, incurring substantial error bars. We summarize the results of our analysis in Table I.

TABLE I. Various quantities for $CaFe_4As_3$ in the SDW and PM phases. Experimental values for the temperature derivative of the thermopower dS/dT (μV/K^2) extrapolated from $T = T_N$ (PM) and $T = T_2$ (SDW) to $T = 0$, the calculated density of states $N(\varepsilon_F)$ (states/eV/Fe), and its energy derivative $N'(\varepsilon_F)$ at the Fermi level (states/eV^2-Fe). γ_g is the measured Sommerfeld coefficient $\gamma_g = (C_p - C_{ph})/T$ (J/Fe-mol K^2), extrapolated to $T = 0$. Z_γ and Z_S are the calculated values of the quasiparticle renormalization determined from measurements of the specific heat and thermopower, respectively (see text).

	$N(\varepsilon_F)$	$N'(\varepsilon_F)$	dS/dT	Z_S	γ_g	Z_γ
SDW ($T \leqslant T_2$)	1.5	12(2)	−0.8(3)	0.16(8)	0.03	0.12
PM ($T \geqslant T_N$)	3.2	−6(2)	0.08(3)	0.37(20)		

The values of Z_S that are extracted from this analysis indicate that $CaFe_4As_3$ is very strongly correlated in the paramagnetic state, and that the quasiparticle mass is more than doubled with the onset of commensurate SDW order, an observation that is echoed in the large Kadowaki-Woods ratio found in the low-temperature Fermi liquid phase. The values of Z_S and Z_γ are in reasonable agreement in the SDW phase, and support the conclusion that the SDW removes less correlated parts of the Fermi surface, leaving quasiparticles that are much more strongly correlated in the SDW phase of $CaFe_4As_3$ than in other members of the iron pnictide families. This is quite different from what is found in other iron pnictide and chalcogenide superconductors, in which the magnetic phases are more coherent and less correlated than the paramagnetic phases. The presence of a large Sommerfeld coefficient implies that the SDW gap Δ does not extend over the entire Fermi surface, although the quasiparticles associated with the ungapped Fermi surface appear to be strongly interacting at the lowest temperatures.

The large value of the Sommerfeld coefficient γ_g in the SDW phase suggests that $CaFe_4As_3$ may have a large value of the Seebeck coefficient via the Behnia-Flouquet ratio[37]

$$\frac{S}{\gamma_g T} = -\frac{3}{\pi^2|e|}\frac{1}{N(\varepsilon_F)}\frac{\Phi'(\varepsilon_F)}{\Phi(\varepsilon_F)}\frac{E_2^1}{E_0^1}. \quad (3)$$

However, we find instead that the thermoelectric power S is small at all temperatures, due to the weak energy dependence of the density of states near the Fermi level. Although we find that $CaFe_4As_3$ has a rather small thermal conductivity κ and as well an electrical resistivity ρ that is somewhat larger than expected in a good metal, perhaps due to the strong quasiparticle interactions implied by the small values of Z, these factors are not sufficient to overcome the small values of S, giving a disappointingly small value for the thermoelectric figure of merit $\mathcal{Z} = S^2/\kappa\rho$ in $CaFe_4As_3$. We find that the largest values of $\mathcal{Z}T$ occur at 200 K, where $\mathcal{Z}T = 1.7 \times 10^{-4}$, indicating that similar thermoelectric performances are found in the high-temperature range in both $CaFe_4As_3$ and some skutterudites, such as $PrFe_4As_{12}$.[9]

Clearly, the figure of merit $\mathcal{Z}$ in $CaFe_4As_3$ is limited by the relatively small thermopower, and Fig. 5 shows that the reason is a surprising particle-hole symmetry that limits $N'(0)$. Provided that the strength of the electronic correlations is not reduced, we believe that electron doping should lead to a considerable enhancement of the thermopower. For instance, the DFT density of states suggests that the thermopower in the paramagnetic state changes sign and increases by about an order of magnitude at the following doping levels: 9–14 % on the Fe site, 12–19 % on the As site, and 35–50 % on the Ca site. However, if many-body renormalizations are included, the required doping levels can be expected to be substantially reduced from the levels predicted by DFT. Similarly, we speculate that superconductivity might be induced in $CaFe_4As_3$ by improving its metallic character, perhaps by a dopant that reduces the lattice constant. Further experimental and theoretical work is needed to establish whether a localized or itinerant picture is more appropriate for $CaFe_4As_3$.

ACKNOWLEDGMENTS

Work at Brookhaven National Laboratory was carried out under the auspices of the U.S. Department of Energy, Office of Basic Energy Sciences, under Contract No. DE-AC02-98CH1886. Work at Rice University and at Rutgers (G.K.) is supported by DoD MURI "Towards New and Better High Temperature Superconductors." Work at Rutgers (Z.Y.) was carried out under the auspices of a DoD National Security Science and Engineering Faculty Fellowship, via AFOSR Grant No. FA 9550-10-1-0191.

[1] G. S. Nolas, J. Sharp, and H. J. Goldsmid, *Thermoelectrics* (Springer, Berlin, 2001).

[2] B. C. Sales, in *Handbook on the Physics and Chemistry of Rare Earths*, edited by K. A. Gschneidner Jr., J.-C. G. Bünzli, and V. K. Pecharsky (North-Holland, Amsterdam, 2003), Vol. 33, p. 1.

[3] T. Takabatake, E. Matsuoka, S. Narazu, K. Hayashi, S. Morimoto, T. Sasakawa, K. Umeo, and M. Sera, Physica B **383**, 93 (2006).

[4] B. C. Sales, D. Mandrus, B. C. Chakoumakos, V. Keppens, and J. R. Thompson, Phys. Rev. B **56**, 15081 (1997).

[5] T. Goto, Y. Nemoto, K. Sakai, T. Yamaguchi, M. Akatsu, T. Yanagisawa, H. Hazama, K. Onuki, H. Sugawara, and H. Sato, Phys. Rev. B **69**, 180511(R) (2004).

[6] I. Todorov, D. Y. Chung, C. D. Malliakas. Q. Li, T. Bakas, A. Douvalis, G. Trimarchi, K. Gray, J. F. Mitchell, A. J. Freeman, and M. G. Kanatzidis, J. Am. Chem. Soc. **131**, 5405 (2009).

[7] L. L. Zhao, T. Yi, J. C. Fettinger, S. M. Kauzlarich, and E. Morosan, Phys. Rev. B **80**, 020404(R) (2009).

[8] A. Watcharapasorn, R. S. Feigelson, T. Calillat, A. Borshchevsky, G. J. Snyder, and J.-P. Fleurial, J. Appl. Phys. **91**, 1344 (2002).

[9] T. A. Sayles, W. M. Yuhasz, J. Paglione, T. Yanagisawa, J. R. Jeffries, M. B. Maple, Z. Henkie, A. Pietraszko, T. Cichorek, R. Wawryk, Y. Nemoto, and T. Goto, Phys. Rev. B **77**, 144432 (2008).

[10]P. Manuel, L. C. Chapon, I. S. Todorov, D. Y. Chung, J.-P. Castellan, S. Rosenkranz, R. Osborn, P. Toledano, and M. G. Kanatzidis, Phys. Rev. B **81**, 184402 (2010).
[11]Y. Nambu, L. L. Zhao, E. Morosan, K. Kim, G. Kotliar, P. Zajdel, M. A. Green, W. Ratcliff, J. A. Rodriguez-Rivera, and C. Broholm, Phys. Rev. Lett. **106**, 037201 (2011).
[12]A. Rudajevová, M. Švantner, D. Vasylyev, O. Musil, and V. Lang, Int. J. Thermophys. **27**, 1241 (2006).
[13]J. Sebek and E. Santava, J. Phys.: Conf. Ser. **150**, 012044 (2009).
[14]S. Narazu, Y. Hadano, T. Takabatake, and H. Sugawara, J. Phys. Soc. Jpn. **77**, 238 (2008).
[15]E. D. Bauer, A. Ślebarski, N. A. Frederick, W. M. Yuhasz, M. B. Maple, D. Cao, F. Bridges, G. Giester, and P. Rogl, J. Phys. Condens. Matter **16**, 5095 (2004).
[16]B. C. Sales, B. C. Chakounmake, and D. Mandrus, J. Solid State Chem. **146**, 528 (1999).
[17]G. S. Nolas, G. A. Slack, D. T. Morelli, T. M. Tritt, and A. C. Ehrlich, J. Appl. Phys. **79**, 4002 (1996).
[18]R. S. Kwok and S. E. Brown, Phys. Rev. Lett. **63**, 895 (1989).
[19]K. Maki, Phys. Rev. B **46**, 7219 (1992).
[20]E. Fawcett, Rev. Mod. Phys. **60**, 209 (1988).
[21]F. J. Blatt, P. A. Schroeder, C. L. Foils, and D. Greig, *Thermopelectric Power of Metals* (Plenum Press, New York, 1976).
[22]M. Matusiak, Z. Bukowski, and J. Karpinski, Phys. Rev. B **81**, 020510 (2010).
[23]F. Ma, Z. Lu, and T. Xiang, Front. Phys. China **5**, 150 (2010).
[24]P. A. Fedders and P. C. Martin, Phys. Rev. **143**, 245 (1966).
[25]S. Murayama, C. Sekine, A. Yokoyanagi, K. Hoshi, and Y. Ōnuki, Phys. Rev. B **56**, 11092 (1997).
[26]L. S. Mazov, Phys. Rev. B **70**, 054501 (2004).
[27]T. Miyake, K. Nakamura, R. Arita, and M. Imada, J. Phys. Soc. Jpn. **79**, 044705 (2010).
[28]J.-X. Zhu, R. Yu, H. D. Wang, L. L. Zhao, M. D. Jones, J. H. Dai, E. Abrahams, E. Morosan, M. H. Fang, and Q. Si, Phys. Rev. Lett. **104**, 216405 (2010).
[29]K. Haule, J. H. Shim, and G. Kotliar, Phys. Rev. Lett. **100**, 226402 (2008).
[30]M. M. Qazilbash, J. J. Hamlin, R. E. Baumbach, Lijun Zhang, D. J. Singh, M. B. Maple, and D. N. Basov, Nature Phys. **5**, 64 (2009).
[31]P. E. Blöchl, Phys. Rev. B **50**, 17953 (1994).
[32]G. Kresse and D. Joubert, Phys. Rev. B **59**, 1758 (1999).
[33]G. Kresse and J. Furthmüller, Phys. Rev. B **54**, 11169 (1996).
[34]J. P. Perdew, K. Burke, and M. Ernzerhof, Phys. Rev. Lett. **77**, 3865 (1996).
[35]G. Pàlsson and G. Kotliar, Phys. Rev. Lett. **80**, 4775 (1998).
[36]K. Haule and G. Kotliar, *Properties and Applications of Thermoelectric Materials*, edited by V. Zlatic and A. C. Hewson (Springer, New York, 2009), p. 119.
[37]K. Behnia, D. Jaccard, and J. Flouquet, J. Phys. Condens. Matter **16**, 5187 (2004).